Langmuir
Article
pubs.acs.org/Langmuir

Examining the Lateral Displacement of HL60 Cells Rolling on Asymmetric P-Selectin Patterns

Chia-Hua Lee,[†,∥] Suman Bose,[‡,∥] Krystyn J. Van Vliet,[†] Jeffrey M. Karp,[§] and Rohit Karnik*[,‡]

[†]*Department of Materials Science and Engineering, and* [‡]*Department of Mechanical Engineering, Massachusetts Institute of Technology, Cambridge, Massachusetts 02139, United States, and* [§]*HST Center for Biomedical Engineering and Harvard Stem Cell Institute, Brigham and Women's Hospital and Harvard Medical School, Cambridge, Massachusetts 02139, United States.* [∥]*These authors contributed equally to the paper*

Received July 19, 2010. Revised Manuscript Received October 15, 2010

The lateral displacement of cells orthogonal to a flow stream by rolling on asymmetrical receptor patterns presents a new opportunity for the label-free separation and analysis of cells. Understanding the nature of cell rolling trajectories on such substrates is necessary to the engineering of substrates and the design of devices for cell separation and analysis. Here, we investigate the statistical nature of cell rolling and the effect of pattern geometry and flow shear stress on cell rolling trajectories using micrometer-scale patterns of biomolecular receptors with well-defined edges. Leukemic myeloid HL60 cells expressing the PSGL-1 ligand were allowed to flow across a field of patterned lines fabricated using microcontact printing and functionalized with the P-selectin receptor, leveraging both the specific adhesion of this ligand−receptor pair and the asymmetry of the receptor pattern inclination angle with respect to the fluid shear flow direction (α = 5, 10, 15, and 20°). The effects of the fluid shear stress magnitude (τ = 0.5, 1, 1.5, and 2.0 dyn/cm^2), α, and P-selectin incubation concentration were quantified in terms of the rolling velocity and edge tracking length. Rolling cells tracked along the inclined edges of the patterned lines before detaching and reattaching on another line. The detachment of rolling cells after tracking along the edge was consistent with a Poisson process of history-independent interactions. Increasing the edge inclination angle decreased the edge tracking length in an exponential manner, contrary to the shear stress magnitude and P-selectin incubation concentration, which did not have a significant effect. On the basis of these experimental data, we constructed an empirical model that predicted the occurrence of the maximum lateral displacement at an edge angle of 7.5°. We also used these findings to construct a Monte Carlo simulation for the prediction of rolling trajectories of HL60 cells on P-selectin-patterned substrates with a specified edge inclination angle. The prediction of lateral displacement in the range of 200 μm within a 1 cm separation length supports the feasibility of label-free cell separation via asymmetric receptor patterns in microfluidic devices.

Introduction

The separation and analysis of cells in a heterogeneous population is important for diagnostic and therapeutic applications and for elucidating the biology of rare cell types. Although the separation of cells is routine using flow cytometry, there exists a growing need for technologies that are less capital-intensive and do not require modification or labeling of the sorted cells. For example, separation methods for therapeutics or the subsequent analysis of cells need to preserve the cell phenotype; point-of-care diagnostics, especially in nonindustrialized settings, also require a simplicity of operation with a minimized number of processing steps. Cell sorting methods based on adhesion are especially promising for these applications because they require minimal cell processing and provide high specificity through ligand−receptor or antibody−antigen interactions.[1−5] Similarly, the observation of cell−surface interactions on immobilized receptors offers the opportunity for the label-free enumeration of cells[2] and the potential for the direct analysis of the cell phenotype or receptor expression.

Devices for label-free cell separation and analysis can leverage in vivo mechanisms of selective and reversible cell adhesion. For example, the rolling of leukocytes, hematopoietic stem cells, and cancer cells along the vasculature under shear flow is mediated by reversible binding between glycoprotein receptors known as selectins (on the vascular endothelial cell surface) and selectin ligands (on the rolling cell surface).[6−11] In contrast to conventional antibody-based methods, separation based on cell rolling

*To whom correspondence should be addressed: Tel 617-324-1155; Fax 617-258-9346; Email: karnik@mit.edu.

(1) Greenberg, A. W.; Kerr, W. G.; Hammer, D. A. Relationship between selectin-mediated rolling of hematopoietic stem and progenitor cells and progression in hematopoietic development. *Blood* **2000**, *95*, 478–486.

(2) Cheng, X. H.; Irimia, D.; Dixon, M.; Sekine, K.; Demirci, U.; Zamir, L.; Tompkins, R. G.; Rodriguez, W.; Toner, M. A microfluidic device for practical label-free CD4+T cell counting of HIV-infected subjects. *Lab Chip* **2007**, *7*, 170–178.

(3) Nagrath, S.; Sequist, L. V.; Maheswaran, S.; Bell, D. W.; Irimia, D.; Ulkus, L.; Smith, M. R.; Kwak, E. L.; Digumarthy, S.; Muzikansky, A.; Ryan, P.; Balis, U. J.; Tompkins, R. G.; Haber, D. A.; Toner, M. Isolation of rare circulating tumour cells in cancer patients by microchip technology. *Nature* **2007**, *450*, 1235–1239.

(4) Tondreau, T.; Lagneaux, L.; Dejeneffe, M.; Delforge, A.; Massy, M.; Mortier, C.; Bron, D. Isolation of BM mesenchymal stem cells by plastic adhesion or negative selection: phenotype, proliferation kinetics and differentiation potential. *Cytotherapy* **2004**, *6*, 372–379.

(5) Narasipura, S. D.; Wojciechowski, J. C.; Charles, N.; Liesveld, J. L.; King, M. R. P-selectin-coated microtube for enrichment of CD34(+) hematopoietic stem and progenitor cells from human bone marrow Hematology. *Clin. Chem.* **2008**, *54*, 77–85.

(6) Bell, G. I. Models for specific adhesion of cells to cells. *Science* **1978**, *200*, 618–627.

(7) Marshall, B. T.; Long, M.; Piper, J. W.; Yago, T.; McEver, R. P.; Zhu, C. Direct observation of catch bonds involving cell-adhesion molecules. *Nature* **2003**, *423*, 190–193.

(8) Alon, R.; Hammer, D. A.; Springer, T. A. Lifetime of the P-selectin-carbohydrate bond and its response to tensile force in hydrodynamic flow. *Nature* **1995**, *374*, 539–542.

(9) Granger, D. N.; Kubes, P. The microcirculation and inflammation - modulation of leukocyte-endothelial cell-adhesion. *J. Leukocyte Biol.* **1994**, *55*, 662–675.

on immobilized receptors obviates labeling and label-removal steps, enabling facile elution with a minimized alteration of viability or function postsorting.[12−14] In addition, co-immobilization of other cell-type-specific molecules along with selectins can significantly influence cell rolling,[15,16] which opens the possibility of further tuning the specificity of separation and analysis on the basis of the expression of a pertinent receptor on the cell.

We recently showed that patterning lines of P-selectin receptors, inclined at an angle to the direction of fluid flow, can be used to direct the trajectories of rolling HL60 cells on the asymmetrically patterned surface; this finding opens the possibility of using microfluidic devices for the simple, continuous-flow, label-free separation and analysis of cells.[17] Such devices have the potential for rapid diagnostic applications including the detection of sepsis and inflammatory conditions that alter cell rolling behavior,[18−20] the separation and enumeration of different leukocytes from blood using ligands with appropriate specificities,[21] and label-free analysis of the expression of cell surface ligands. Because cell rolling is noninvasive and mimics the natural cell homing process, these devices are also promising for the separation and analysis of subpopulations of hematopoietic or mesenchymal stem cells and the enrichment of circulating rare cells.[5,16]

Figure 1a schematizes a separation device that employs cell rolling on receptor-patterned substrates to sort cell populations in a single step. Figure 1b shows the trajectories of a cell rolling within such a patterned device substrate. Cells that track along the edges of these patterns are laterally displaced into the adjacent buffer stream, resulting in separation. A quantitative understanding of the nature of cell rolling trajectories and lateral displacements on receptor-patterned substrates is a prerequisite to the realization of such devices. Our earlier study demonstrated that HL60 cells could track along P-selectin edges;[17] however, the effect of flow conditions and the pattern inclination angle on cell rolling trajectories was not studied. Furthermore, the distribution of edge tracking lengths and lateral displacements was not analyzed because of insufficient data obtained from a single patterned edge. Therefore, how the parameters of cell rolling relate to cell rolling trajectories and lateral displacements for such asymmetrical patterns is poorly understood. For example, it is unknown to what extent cell rolling is affected by shear stress magnitudes or pattern inclination angles. Furthermore, the nature of the detachment of cells after tracking along an edge is not known, and is it not yet established whether the detachment of cells from such patterns is a random process that is unaltered by the history of interaction with the pattern itself. A systematic study of cell rolling trajectories along such well-defined receptor patterns is therefore a prerequisite to addressing these issues and enabling the development of label-free devices for the separation or analysis of cells such as the device envisioned in Figure 1.

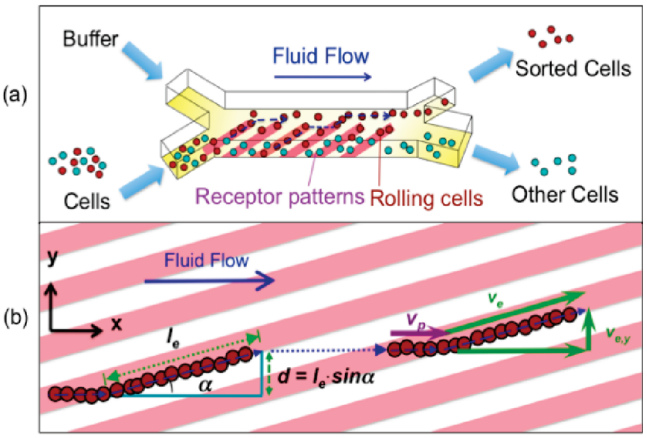

Figure 1. (a) Schematic diagram of a device for the separation of cells. Cells rolling along patterned edges are laterally displaced into the adjacent buffer stream, resulting in separation. Pink lines indicate receptor-functionalized regions. Red and blue circles are cells that do and do not, respectively, express ligands that bind specifically to those receptors. (b) Illustration of a typical cell rolling trajectory along the receptor pattern inclined at an angle of α to the fluid flow direction. The cell binds within the receptor line and rolls in the direction of shear flow toward the pattern edge. The cell then tracks the edge to define an edge tracking length l_e, resulting in a net lateral displacement d, before detaching to continue along the direction of fluid flow before possible reattachment and rolling along a new receptor line. The cell rolling velocity v_p within the receptor-functionalized line in the x direction of fluid flow can be distinguished from the velocity v_e along the line edge, where $v_{e,y}$ is the lateral velocity (the vertical component perpendicular to the streamlines and parallel to the lateral displacement, d).

In this work, we quantify cell rolling trajectories and study the effect of pattern geometry, shear stress, and P-selectin incubation concentration on the rolling of HL60 cells, which are widely used as a model to study leukocyte rolling.[12,22−25] HL60 cell surfaces express a specific ligand termed P-selectin glycoprotein ligand-1 (PSGL-1),[22] which binds reversibly to the P-selectin receptor to enable rolling in vivo and in vitro. We first developed a technique based on microcontact printing (μCP) to pattern alternating micrometer-scale lines of adhesive P-selectin regions with passivating

(10) Lasky, L. A. Selectin-carbohydrate interactions and the initiation of the inflammatory response. *Annu. Rev. Biochem.* **1995**, *64*, 113–139.
(11) Tedder, T. F.; Steeber, D. A.; Chen, A.; Engel, P. The selectins - vascular adhesion molecules. *FASEB J.* **1995**, *9*, 866–873.
(12) Chang, W. C.; Lee, L. P.; Liepmann, D. Biomimetic technique for adhesion-based collection and separation of cells in a microfluidic channel. *Lab Chip* **2005**, *5*, 64–73.
(13) Greenberg, A. W.; Hammer, D. A. Cell separation mediated by differential rolling adhesion. *Biotechnol. Bioeng.* **2001**, *73*, 111–124.
(14) Nalayanda, D. D.; Kalukanimuttam, M.; Schmidtke, D. W. Micropatterned surfaces for controlling cell adhesion and rolling under flow. *Biomed Microdev.* **2007**, *9*, 207–214.
(15) Chen, S. Q.; Alon, R.; Fuhlbrigge, R. C.; Springer, T. A. Rolling and transient tethering of leukocytes on antibodies reveal specializations of selectins. *Proc. Natl. Acad. Sci. U.S.A.* **1997**, *94*, 3172–3177.
(16) Charles, N.; Liesveld, J. L.; King, M. R. Investigating the feasibility of stem cell enrichment mediated by immobilized selectins. *Biotechnol. Prog.* **2007**, *23*, 1463–1472.
(17) Karnik, R.; Hong, S.; Zhang, H.; Mei, Y.; Anderson, D. G.; Karp, J. M.; Langer, R. Nanomechanical control of cell rolling in two dimensions through surface patterning of receptors. *Nano Lett* **2008**, *8*, 1153–1158.
(18) Ibbotson, G. C.; Doig, C.; Kaur, J.; Gill, V.; Ostrovsky, L.; Fairhead, T.; Kubes, P. Functional alpha4-integrin: a newly identified pathway of neutrophil recruitment in critically ill septic patients. *Nat. Med.* **2001**, *7*, 465–470.
(19) Davenpeck, K. L.; Brummet, M. E.; Hudson, S. A.; Mayer, R. J.; Bochner, B. S. Activation of human leukocytes reduces surface P-selectin glycoprotein ligand-1 (PSGL-1, CD162) and adhesion to P-selectin in vitro. *J. Immunol.* **2000**, *165*, 2764–2772.
(20) Lorant, D. E.; Mcever, R. P.; Mcintyre, T. M.; Moore, K. L.; Prescott, S. M.; Zimmerman, G. A. Activation of polymorphonuclear leukocytes reduces their adhesion to P-selectin and causes redistribution of ligands for p-selectin on their surfaces. *J. Clin. Invest.* **1995**, *96*, 171–182.
(21) Reinhardt, P. H.; Kubes, P. Differential leukocyte recruitment from whole blood via endothelial adhesion molecules under shear conditions. *Blood* **1998**, *92*, 4691–4699.
(22) Norman, K. E.; Moore, K. L.; Mcever, R. P.; Ley, K. Leukocyte rolling in vivo is mediated by P-Selectin glycoprotein ligand-1. *Blood* **1995**, *86*, 4417–4421.
(23) Lawrence, M. B.; Kansas, G. S.; Kunkel, E. J.; Ley, K. Threshold levels of fluid shear promote leukocyte adhesion through selectins (CD62L,P,E). *J. Cell Biol.* **1997**, *136*, 717–727.
(24) Dong, C.; Lei, X. X. Biomechanics of cell rolling: shear flow, cell-surface adhesion, and cell deformability. *J. Biomech.* **2000**, *33*, 35–43.
(25) Wu, L.; Xiao, B. T.; Jia, X. L.; Zhang, Y.; Lu, S. Q.; Chen, J.; Long, M. Impact of carrier stiffness and microtopology on two-dimensional kinetics of P-selectin and P-selectin glycoprotein ligand-1 (PSGL-1) interactions. *J. Biol. Chem.* **2007**, *282*, 9846–9854.

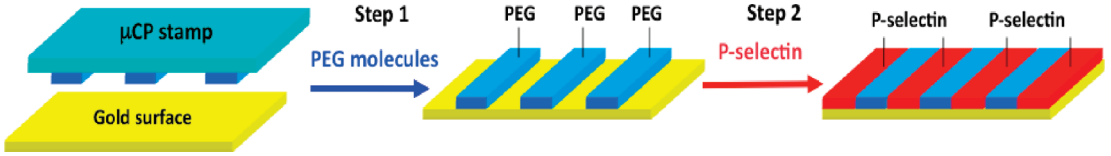

Figure 2. Schematic diagram for patterning P-selectin on a gold substrate involving microcontact printing. Step 1: Selective deposition of PEG molecules onto the gold surface. Step 2: Filling in of the uncoated surface with P-selectin.

poly(ethylene glycol) regions on a gold substrate. We then quantified the edge tracking lengths and rolling velocities of HL60 cells along these patterned substrates within a flow chamber at different edge inclination angles, shear stress magnitudes and P-selectin incubation concentrations. The distribution of edge tracking lengths and the observation of the reattachment of cells were incorporated into a computational simulation tool to predict the trajectories of cells on a patterned substrate.

Materials and Methods

Materials. Gold-coated glass slides were purchased from EMF Corp. All slides were cleaned with piranha solution prior to use (3:1 mixture of sulfuric acid (Sigma-Aldrich) and 30% hydrogen peroxide (Sigma-Aldrich)). 1-Mercaptoundec-11-yl-tetra(ethylene glycol) (PEG alkanethiol, Sigma-Aldrich) was diluted in absolute ethanol (Pharmco-AAPER) to a concentration of 5 mM for microcontact printing. Recombinant human P-selectin (R&D Systems Inc.) and bovine serum albumin (BSA, Rockland Immunochemicals, Inc.) were diluted in 150 mM NaCl Dulbecco's phosphate-buffered saline (DPBS, Mediatech Inc.). All materials employed in this study were used without further purification unless specified.

PDMS Stamps. Microcontact printing stamps that defined the receptor pattern were fabricated in poly(dimethylsiloxane) (PDMS) using an SU-8 molding process. The small line-patterned stamp (SS) (15 μm line width and 10 μm spacing between adjacent lines) and the large line-patterned stamp (LS) (70 μm stamping regions spaced 50 μm apart) were used to characterize the patterning process and cell rolling behavior, respectively.

Fabrication of Patterned Substrates. A schematic diagram of the patterning process is shown in Figure 2. Step 1: Microcontact printing (μCP) was used to form alternating self-assembled monolayers (SAMs) of PEG molecules on the gold substrate. The PDMS stamp was first inked with PEG solution in ethanol (5 mM), dried, and pressed onto the surface to be patterned for 40 s. The surface was then rinsed with ethanol and dried under a stream of N_2 (Figure 3a,c). Step 2: After the selective deposition of PEG molecules, the substrates were incubated in P-selectin solution (15 μg/mL in DPBS, unless stated otherwise) using a perfusion chamber (Electron Microscopy Sciences) for 3 h at room temperature to pattern the remaining areas with P-selectin (Figure 3b,d). The surfaces were then backfilled with BSA (1 mg/mL in DPBS) for 1 h to block nonspecific interactions.

Substrate Characterization. Atomic force microscopy (Veeco Dimension 3100, tapping mode, 1 Hz scan rate) and scanning electron microscopy (JEOL 6700, 3.5 kV acceleration voltage) were used to characterize the patterned surface geometry. All substrates for AFM and SEM characterization were placed in a vacuum chamber overnight before imaging to minimize residual solvent on the surface; no further coating was employed for SEM imaging.

Cell Culture. HL60 myeloid cells (obtained from ATCC) were maintained in Iscove's modified Dulbecco's medium supplemented with 20% fetal bovine serum according to the ATCC recommendation. Cells were cultured in 75 cm^2 polystyrene tissue culture flasks (BD Falcon) with the cell density maintained between 10^5–10^6 cells/mL (with passage numbers 26, 27, and 29 used in the study of the effect of the inclination angle and shear stress, and with passage numbers 23, 24, and 25 used in the study of the effect of P-selectin incubation concentration).

Cell Rolling Experiments in a Flow Chamber. A suspension of HL60 cells (~10^5 cells/mL) was allowed to flow over the patterned surfaces in a rectangular flow chamber (Glycotech, Inc.; width w = 1.0 cm, length l = 6 cm, and height h = 0.005 in.) with inclination angles of the receptor pattern of α = 5, 10, 15, or 20° at a room temperature of 24.5 °C. A syringe pump (World Precision Instruments (WPI), SP230IW) was used to generate different flow rates of between 75 and 300 μL/min, with corresponding shear stresses of 0.5–2.0 dyn/cm^2 (~0.05–0.2 Pa). The flow was laminar (Reynold's number $Re \approx 0.1$–3), and the shear stress τ was calculated using the plane Poiseuille flow equation $\tau = 6\mu Q/wh^2$, where μ is the kinematic viscosity, Q is the volumetric flow rate, w is the width of the flow chamber, and h is the height of the flow chamber. An inverted microscope (Nikon TE2000-U) with a mounted camera (Andor iXon 885) was used to record HL60 rolling interactions with adhesive P-selectin substrates using a 4× objective, typically at a rate of 1 frame/s for a duration of 300 s. For each shear stress magnitude and pattern inclination angle, three independent experiments were performed. Data are presented as the mean and the standard deviation of the average values obtained from each experiment.

Data Analysis. *Tracking of Cells*. The image sequences were analyzed using a customized Matlab (Mathworks, Inc.) program that utilized particle-tracking freeware[26] to detect the cells and generate tracks along the patterned line edges. The procedure used to generate tracks has been described in our earlier work.[27] We set a tracking criterion that required the cell displacement between consecutive frames to be less than 10 μm. Tracks with a total length of < 40 μm were not included in the analysis of the distribution of cell responses because these short tracks predominantly represented artifacts on the substrate such as pinholes and in some cases unlinked fragments of a single track. These settings allowed for the selective tracking of only the rolling cells because the velocities of the nonadhered freely flowing cells were much higher (Figure 4). Tracks generated by the software were randomly selected and manually inspected by comparison with the images to ascertain their accuracy.

Identification of Tracks That Encountered an Edge. The positions of the patterned edges were identified using the difference in contrast between the PEG and P-selectin regions as imaged using optical microscopy. Tracks with end points within 10 μm of the nearest edge were identified as having encountered an edge.

Identification of the Portion of a Track Representing Cell Rolling along the Edge. Two intersecting straight lines were fitted to every selected track—one aligned with the flow direction and the other aligned with the edge. A constrained error minimization scheme with the slopes of the two lines and the intersection point (P_i) as the fitting parameter was used. Although the slopes of the two lines were allowed to vary ±3° from the flow direction and the angle of the pattern, their intersection point was confined such that the x and y coordinates of the intersection point were within the limits of the minimum and maximum values of the x and y coordinates of the points on the track. Thus, the

(26) http://physics.georgetown.edu/matlab/.
(27) Karnik, R.; Hong, S.; Zhang, H.; Mei, Y.; Anderson, D. G.; Karp, J. M.; Langer, R. Nanomechanical control of cell rolling in two dimensions through surface Patterning of receptors. *Nano Lett.* **2008**, *8*, 1153–1158.

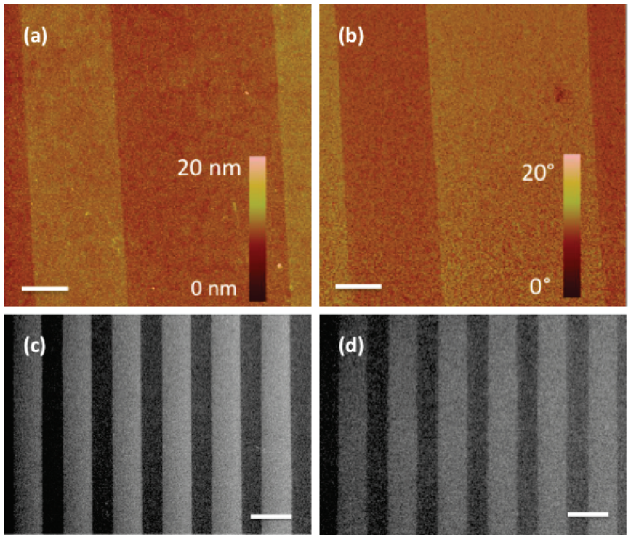

Figure 3. Characterization of P-selectin patterned substrates for cell rolling. AFM images of 10-μm-wide P-selectin lines separated by 15-μm-wide PEG bands (after step 2), displaying the contrast between P-selectin and PEG regions in (a) height and (b) phase, respectively. The phase image indicates a difference between the mechanical properties of the surface in the two regions. SEM images of surfaces (c) after PEG printing (step 1) and (d) after P-selectin adsorption (step 2), respectively, showing patterning uniformity (with brighter areas corresponding to PEG regions). Scale bars are (a, b) 5 μm and (c, d) 100 μm.

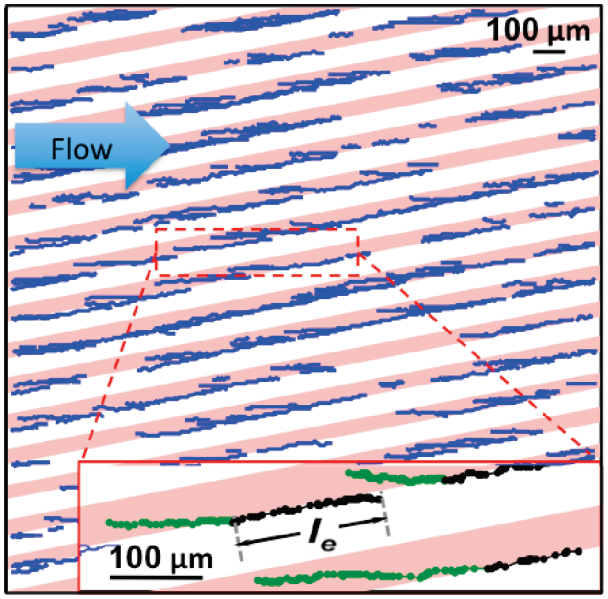

Figure 4. Tracks of HL60 cells rolling (blue lines) on P-selectin lines (pink) were obtained by analyzing 300 images acquired at 1 fps using a customized Matlab code. The edge inclination angle was 10°, and the shear stress was 0.5 dyn/cm^2. The inset shows a track corresponding to a cell that first rolled inside the P-selectin line (green) in the direction of fluid flow and then tracked along the edge (black).

tracks were subdivided into two segments—one that represented rolling inside the P-selectin line and another that represented rolling on the edge (Figure 1b, inset).

Extraction of Edge Tracking Length, l_e. The length traveled along the patterned line edge was calculated from the distance between P_i and the end of the track. To avoid biasing the population, tracks that were restricted by space (field of view of the camera) or time (tracks that existed before or continued after the image sequence) or tracks that rolled only on the edge without a segment of track on the band (distance of < 10 μm between the intersection point P_i and the beginning of the track) were excluded from the calculation of the average edge tracking length.

Extraction of Rolling Velocities on the Edge and within the P-Selectin Lines. The velocity was calculated by choosing two points on the track and dividing the distance between the points by the time taken to traverse them. We observed that the rolling velocity was smaller around P_i when a cell transitioned from rolling within the P-selectin line to rolling along the edge. We therefore excluded the portion of the track that was within a distance of 10 μm from the predicted P_i for the calculation of rolling velocities. Thus, the starting point and the point located 10 μm before P_i were used to calculate the rolling velocity v_p within the patterned lines, and the point located 10 μm ahead of P_i and the end point of the track were used to calculate the velocity v_e along the edge of the patterned lines. Tracks that did not encounter the patterned edge were used only to calculate v_p, and tracks that were confined only to the edge (segment of < 10 μm on the band) were used only to calculate v_e, each by taking the ratio of the total track length to the total elapsed time. Thus, for each experiment an array of the edge tracking length, velocity on the edge, and velocity in a plain region was generated and used for further analysis.

Measuring the Lateral Displacement of Cells over Multiple Edges. To track cells as they detached from one edge and reattached downstream, an algorithm was developed to join tracks of cells on consecutive bands by searching for a new track that appeared downstream from the location at which a cell detached from an edge. On the basis of the point at which a cell detached, the trajectory of the free-flowing cell was predicted on the basis of the flow direction and velocity. Downstream tracks that started within 20 μm of the predicted trajectory in the following frame were considered to be continuations of the former track and were joined together. The accuracy of the joining algorithm was confirmed by manually comparing the tracks with the image sequences. Finally, for each of the tracks the lateral displacement after traveling along three consecutive edges was recorded.

Simulation of Cell Rolling Trajectories. A Monte Carlo simulation of cell rolling on a substrate patterned with P-selectin lines with edge inclination angle α was performed by assuming that the cell detachment from the edge followed a Poisson distribution. The value of λ for the Poisson distribution corresponding to the edge inclination angle α was obtained as described in Results and Discussion. The direction of fluid flow was along the positive x direction, and the cells were assumed to roll on all P-selectin lines that they encountered. For each cell, the edge tracking length was calculated by generating a random number based on the Poisson distribution by inverse transform sampling, and the position of the cell was correspondingly updated. The cell was then assumed to detach and begin rolling on the next downstream edge at the same y coordinate. For the case in which the lateral displacement of the cell after rolling on three edges was desired, the process was repeated three times and the net change in the y coordinate (net lateral displacement) was stored. To simulate the cell trajectories when they travel a fixed length inside a separation device, the above algorithm was repeated with the cell starting at (0, 0) on the first edge until the x-coordinate of the cell was equal to the travel distance, which yielded a final y coordinate (net lateral displacement). The above sequence was iterated for 10^5 cells, and the final y positions of all cells were used to calculate the probability density.

Results and Discussion

Direct microcontact printing (μCP) of proteins has been used widely to control the geometry of protein patterns on various planar surfaces,[28−33] including the printing of P-selectin to study neutrophil rolling.[34] However, it is possible that the protein will denature or lose bioactivity during PDMS stamping steps.[35]

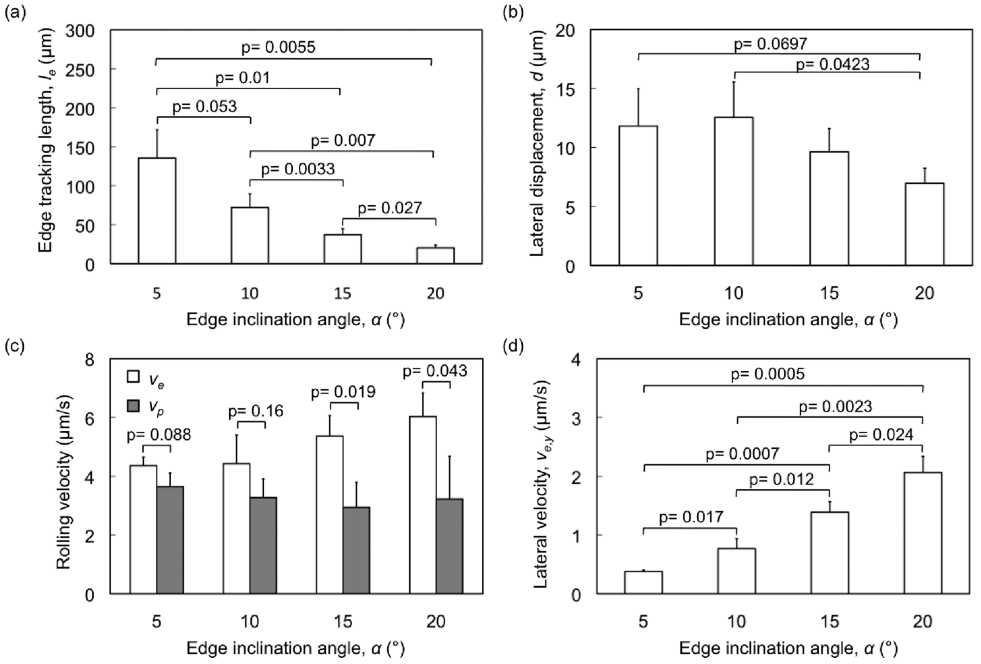

Figure 5. Effect of edge inclination angle α on the rolling behavior of HL60 cells at a fluid shear stress magnitude of 0.5 dyn/cm^2 and P-selectin incubation concentration of 15 μg/mL. Variation of the (a) edge tracking length, l_e; (b) lateral displacement, d; (c) rolling velocities, v_p and v_e, within the P-selectin lines and on the edge, respectively; and (d) lateral velocity, $v_{e,y}$, which is a component of the edge rolling velocity in the direction of lateral displacement. Error bars represent one standard deviation, where $n = 3$ replicate experiments for each condition.

Additionally, the transfer of the stamp material (PDMS) from the stamp to the surface during μCP can contaminate the patterned areas.[36] In the present method, after the selective deposition of PEG molecules, the gold substrate is patterned with P-selectin in the solution phase so that the possibility of denaturation due to protein drying can be ruled out. AFM images of P-selectin patterned using the small line-patterned stamp (SS) show clearly defined 10-μm-wide lines of P-selectin with well-resolved, straight edges (Figure 3a,b). The large line-patterned stamp (LS) was used to prepare surfaces for cell rolling experiments. The sharp contrast between P-selectin regions and PEG regions confirms that the resulting patterns had well-defined edges over large areas as revealed by SEM (Figure 3c,d). In addition to this surface characterization, we observed that HL60 cells exhibited rolling specifically in the P-selectin patterned regions with velocities in a similar range to those reported in other studies.[27] These results confirm that the PEG-functionalized regions on either side of P-selectin lines could block P-selectin adsorption (as expected from the nonfouling property of PEG) and that P-selectin molecules retained their activity after being adsorbed onto the exposed gold. In addition, we performed experiments to characterize cell adhesion on PEG surfaces and surfaces coated with BSA and did not observe any cell−surface interactions, further confirming that the observed interactions were due to P-selectin.

The P-selectin patterned substrates were incorporated into a flow chamber to study the rolling behavior of HL60 cells at different edge inclination angles, shear stress magnitudes and P-selectin incubation concentration. Figure 4 shows an example of the actual tracks of HL60 cells rolling on P-selectin patterns at an edge angle of 10° and a shear stress of 0.5 dyn/cm^2 and P-selectin incubation concentration of 15 μg/mL. The tracks clearly depict the change in direction of rolling HL60 cells that occurred when the cells encountered the asymmetric edges (movie available in Supporting Information).

Effect of the Edge Angle on the Rolling Behavior of HL60 Cells. We first examined the effect of the edge inclination angle α subtended by edges of the P-selectin lines with respect to the direction of fluid flow on the edge tracking length l_e, the lateral displacement d, and the rolling velocities v_p and v_e. At α = 5°, HL60 cells rolled an average distance of more than 135 μm along the edges before detachment at a shear stress of 0.5 dyn/cm^2 and P-selectin incubation concentration of 15 μg/mL. Figure 5a shows that as the edge angle was increased from 5° to 20° in 5° increments the average edge tracking length l_e decreased significantly (ANOVA, $F = 18.403$, $p = 0.001$). In other words, the ability of the cells to roll along the edges was reduced with increasing edge inclination angle (and increasing component of the fluid force on the cell directed away from the edge). A comparison of data pairs (posthoc t test) demonstrated statistically significant differences in l_e for every 5° increase in α. In contrast, Figure 5b shows that the lateral displacement $d = l_e \sin \alpha$ did not show a significant trend with increasing α (ANOVA, $F = 3.075$, $p = 0.091$) and varied from 7.0 to 12.5 μm over this range of α. However, a

(28) James, C. D.; Davis, R. C.; Kam, L.; Craighead, H. G.; Isaacson, M.; Turner, J. N.; Shain, W. Patterned protein layers on solid substrates by thin stamp microcontact printing. *Langmuir* **1998**, *14*, 741–744.
(29) Bernard, A.; Delamarche, E.; Schmid, H.; Michel, B.; Bosshard, H. R.; Biebuyck, H. Printing patterns of proteins. *Langmuir* **1998**, *14*, 2225–2229.
(30) Tan, J. L.; Tien, J.; Chen, C. S. Microcontact printing of proteins on mixed self-assembled monolayers. *Langmuir* **2002**, *18*, 519–523.
(31) Graber, D. J.; Zieziulewicz, T. J.; Lawrence, D. A.; Shain, W.; Turner, J. N. Antigen binding specificity of antibodies patterned by microcontact printing. *Langmuir* **2003**, *19*, 5431–5434.
(32) Foley, J. O.; Fu, E.; Gamble, L. J.; Yager, P. Microcontact printed antibodies on gold surfaces: Function, uniformity, and silicone contamination. *Langmuir* **2008**, *24*, 3628–3635.
(33) Ghosh, M.; Alves, C.; Tong, Z.; Tettey, K.; Konstantopoulos, K.; Stebe, K. J. Multifunctional surfaces with discrete functionalized regions for biological applications. *Langmuir* **2008**, *24*, 8134–8142.
(34) Lee, D.; King, M. R. Microcontact printing of P-selectin increases the rate of neutrophil recruitment under shear flow. *Biotechnol. Prog.* **2008**, *24*, 1052–1059.
(35) Folch, A.; Toner, M. Microengineering of cellular interactions. *Annu. Rev. Biomed. Eng.* **2000**, *2*, 227–256.
(36) Glasmastar, K.; Gold, J.; Andersson, A. S.; Sutherland, D. S.; Kasemo, B. Silicone transfer during microcontact printing. *Langmuir* **2003**, *19*, 5475–5483.

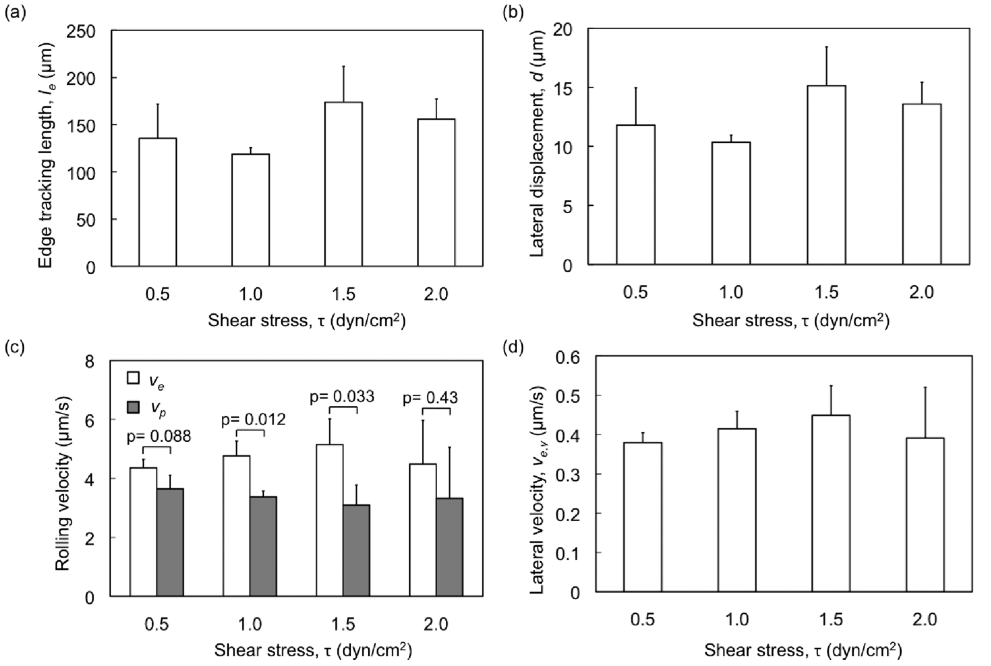

Figure 6. Effect of shear stress τ on the rolling behavior of HL60 cells at an edge inclination angle of 5°. Variation of the (a) edge tracking length, l_e; (b) lateral displacement, d; (c) rolling velocities, v_p and v_e, within the P-selectin lines and on the edge, respectively; and (d) lateral rolling velocity, $v_{e,y}$. Error bars represent one standard deviation, where $n = 3$ replicate experiments for each condition.

statistically significant difference was observed between the lateral displacements at α=10 and 20° (post hoc t test). This behavior can be understood in that although sinα increases with increasing edge inclination angle, edge tracking length l_e concomitantly decreases. It is the magnitude of this lateral displacement that is more relevant to the separation of cells by rolling on such a patterned substrate.

In addition to altering the direction of cell rolling, asymmetric receptor patterns can also alter the rolling velocity of the cells.[27] To examine the effect of α on the rolling velocity, we quantified the average rolling velocity of cells within and along the edges of the P-selectin lines as a function of α at a fixed shear stress magnitude of 0.5 dyn/cm^2 (Figure 5c). The rolling velocity within the P-selectin line was in the range of $v_p = 2.9-3.6$ μm/s and was always less than that along the edge regions ($v_p = 4.4-6.0$ μm/s). This can be understood in terms of the expectation that as α increases, the surface area of interaction and the adhesion resistance to rolling between the cell and the surface decrease, leading to an increase in rolling velocity. Pairwise (t test) statistical analyses show a significant increase in v_e at large edge angles (15 and 20°) compared to v_p, consistent with previous observations.[27] The average rolling velocity on the edge, v_e, increased from 4.4 μm/s for an edge inclination angle of 5° to 6.0 μm/s for an edge inclination angle of 20°, though this trend was not statistically significant (ANOVA, $F = 3.55$, $p = 0.067$). In contrast, $v_{e,y}$ (lateral velocity, defined previously as the edge velocity component in the direction of lateral displacement d) increased significantly from 0.4 to 2.1 μm/s as α increased from 5 to 20°. Thus, receptor patterns characterized by large edge inclination angles (α = 15 and 20°) led to the greater lateral displacement of cells over a given rolling duration.

Effect of Shear Stress on the Rolling Behavior of HL60 Cells. We next examined the effect of shear stress ($\tau = 0.5-2.0$ dyn/cm^2) on the rolling behavior of HL 60 cells. Figure 6 summarizes the edge tracking length, lateral displacement, and rolling velocity of as a function of τ at a fixed edge angle of 5°. The edge tracking length l_e varied in the range of 118.6−173.1 μm over $\tau = 0.5-2.0$ dyn/cm^2. However, there was no statistically significant effect of shear stress on l_e (ANOVA, $F = 2.119$, $p = 0.176$) (Figure 6a). The lateral displacement d varied between 10.3 and 15.1 μm, again with no statistically significant dependence on the shear stress (Figure 6b). Similarly, Figure 6c shows that the rolling velocity within the P-selectin lines and on the edge also did not vary significantly with shear stress (ANOVA, $p = 0.917$ and 0.165, respectively). This lack of dependence on shear stress is not surprising, given that cell rolling involves mechanisms at the cellular and molecular levels to regulate the rolling response over a range of shear stress.[37] Similar independence of the rolling velocity with shear stress has been observed before in the case of HL60 cells rolling on E-selectin:[15] the rolling velocity of HL60 cells has been observed to increase with shear stress at low shear stress ($\tau < 0.5$ dyn/cm^2) and reach a plateau at higher shear stress. Our experiments indicate that, similar to rolling within the P-selectin line, shear stress also does not have a significant effect on the rolling behavior of HL60 cells on asymmetrically patterned edges within $\tau = 0.5-2.0$ dyn/cm^2.

Effect of P-Selectin Incubation Concentration on the Rolling Behavior of HL60 Cells. Apart from the shear stress and edge inclination angle, the P-selectin density on the surface may be expected to affect the trajectories of cells rolling on the inclined edges. Increasing P-selectin density on a glass surface under high shear stress (~20 dyn/cm^2) has been observed to decrease the rolling velocity of HL60 cells, but the receptor density did not modulate the rolling velocity under low shear stress (< 2 dyn/cm^2).[24] When the P-selectin incubation concentration was varied in the range of 5 to 30 μg/mL while maintaining an incubation time of 3 h, we observed no adhesion (5 and 10 μg/mL), nonuniform rolling (11, 12, 13, and 14 μg/mL), robust rolling (15, 20, and 25 μg/mL), and firm adhesion at 30 μg/mL for a shear stress of 0.5 dyn/cm^2. Thus, the range of P-selectin

(37) Yago, T.; Leppanen, A.; Qiu, H. Y.; Marcus, W. D.; Nollert, M. U.; Zhu, C.; Cummings, R. D.; McEver, R. P. Distinct molecular and cellular contributions to stabilizing selectin-mediated rolling under flow. *J. Cell Biol.* **2002**, *158*, 787–799.

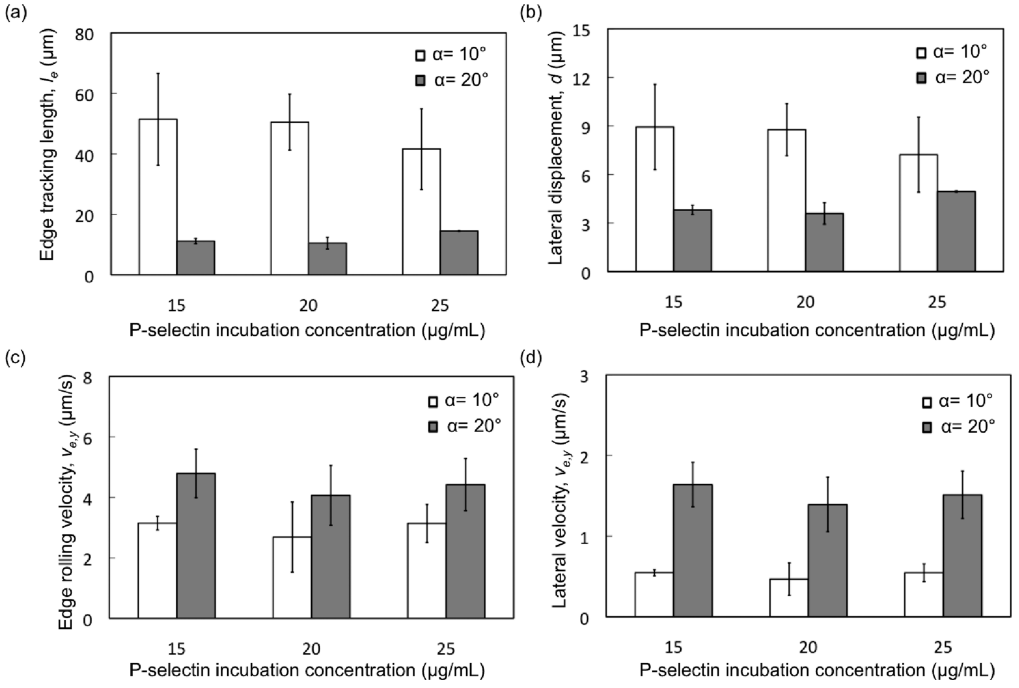

Figure 7. Effect of P-selectin incubation concentration on the rolling behavior of HL60 cells at a shear stress of 0.5 dyn/cm^2. Variation of the (a) edge tracking length, (b) lateral displacement, (c) edge rolling velocity, and (d) lateral velocity with P-selectin incubation concentration at edge inclination angles of $\alpha = 10$ and 20°.

incubation concentration that resulted in a useful rolling response was 15 to 25 μg/mL. We therefore characterized the edge tracking length and cell rolling velocities in this range of P-selectin concentrations. Interestingly, we did not observe a significant change in the rolling velocity with the change in P-selectin incubation concentration: the average rolling velocities inside the bands (v_p) were 2.78 ± 0.57, 2.44 ± 0.64, and 2.67 ± 0.67 μm/s for P-selectin concentrations of 15, 20, and 25 μg/mL at a shear stress of 0.5 dyn/cm^2, respectively. Similarly, we did not observe significant changes in the cell behavior along the edge including the edge tracking length l_e, lateral displacement d, edge rolling velocity v_e, and lateral velocity $v_{e,y}$. These results are in agreement with a previous observation of only a small change in rolling behavior with variation in ligand density under low shear stress (< 2 dyn/cm^2) by Dong et al.[24] These results indicate that when P-selectin is directly immobilized on a gold substrate, the rolling behavior along the edge cannot be controlled as easily by changing P-selectin incubation concentration as that by changing the edge inclination angle.

Detachment of Cells Rolling along an Edge can be Described by a Poisson Process. While the average edge tracking length and lateral displacement are useful in elucidating the effects of the edge inclination angle, shear stress, and P-selectin incubation concentration on cell rolling, a knowledge of the distributions of the distance rolled along the edge and the lateral displacement is important in predicting the eventual spatial distribution of cells in a separation device. Similarly, this knowledge is required to elucidate the number of edge tracking events that must be observed to distinguish between cell phenotypes by observing rolling on the patterned substrates. We therefore examined the distribution of the edge tracking lengths with the aim of developing a model that would serve as a tool to predict cell rolling trajectories and their spread, with direct implications on analysis resolution and separation efficiency.

We observed that for all the experiments conducted, distributions of the edge tracking length exhibited a decaying exponential characteristic similar to that of a Poisson process (Figure 8). A Poisson process occurs when individual events within the process are random in nature and have a uniform probability of occurrence independent of history. It is well known that cell rolling is a stochastic process involving discrete adhesive interactions between the cell and the surface.[38−41] Rolling cells continuously form adhesive contacts with the surface with receptors localized at the tips of extensible structures known as microvilli.[42] As the cell tracks along an edge, new cell-surface adhesions are continuously formed in the region of overlap between the cell's contact area and the receptor-coated region. The cell will detach from the surface when a new adhesive interaction fails to form before the last adhesive interaction is broken under shear flow. If the probability of formation of new adhesive interactions in a given period is constant (i.e., independent of the past rolling history of each cell and/or uncorrelated among cells within a population), then detachment is expected to be a random event and the distance traveled by each cell along the edge is expected to follow a Poisson distribution. To test this hypothesis, we calculated the cumulative distribution function (CDF) from the data and fit it with a Poisson distribution (Figure 7) given by

$$C(l_e) = 1 - \exp(-l_e/\lambda) \quad (1)$$

Here, λ is the mean value of the Poisson distribution. In the ideal case where detachment is a random process, λ will approach

(38) Smith, M. J.; Berg, E. L.; Lawrence, M. B. A direct comparison of selectin-mediated transient, adhesive events using high temporal resolution. *Biophys. J.* **1999**, *77*, 3371–3383.
(39) Chang, K. C.; Hammer, D. A. Adhesive dynamics simulations of sialyl-Lewis(x)/E-selectin-mediated rolling in a cell-free system. *Biophys. J.* **2000**, *79*, 1891–1902.
(40) Jadhav, S.; Eggleton, C. D.; Konstantopoulos, K. A 3-D computational model predicts that cell deformation affects selectin-mediated leukocyte rolling. *Biophys. J.* **2005**, *88*, 96–104.
(41) Korn, C. B.; Schwarz, U. S. Dynamic states of cells adhering in shear flow: from slipping to rolling. *Phys. Rev. E* **2008**, *77*, 041904.
(42) Shao, J. Y.; Hochmuth, R. M. Micropipette suction for measuring piconewton forces of adhesion and tether formation from neutrophil membranes. *Biophys. J.* **1996**, *71*, 2892–2901.

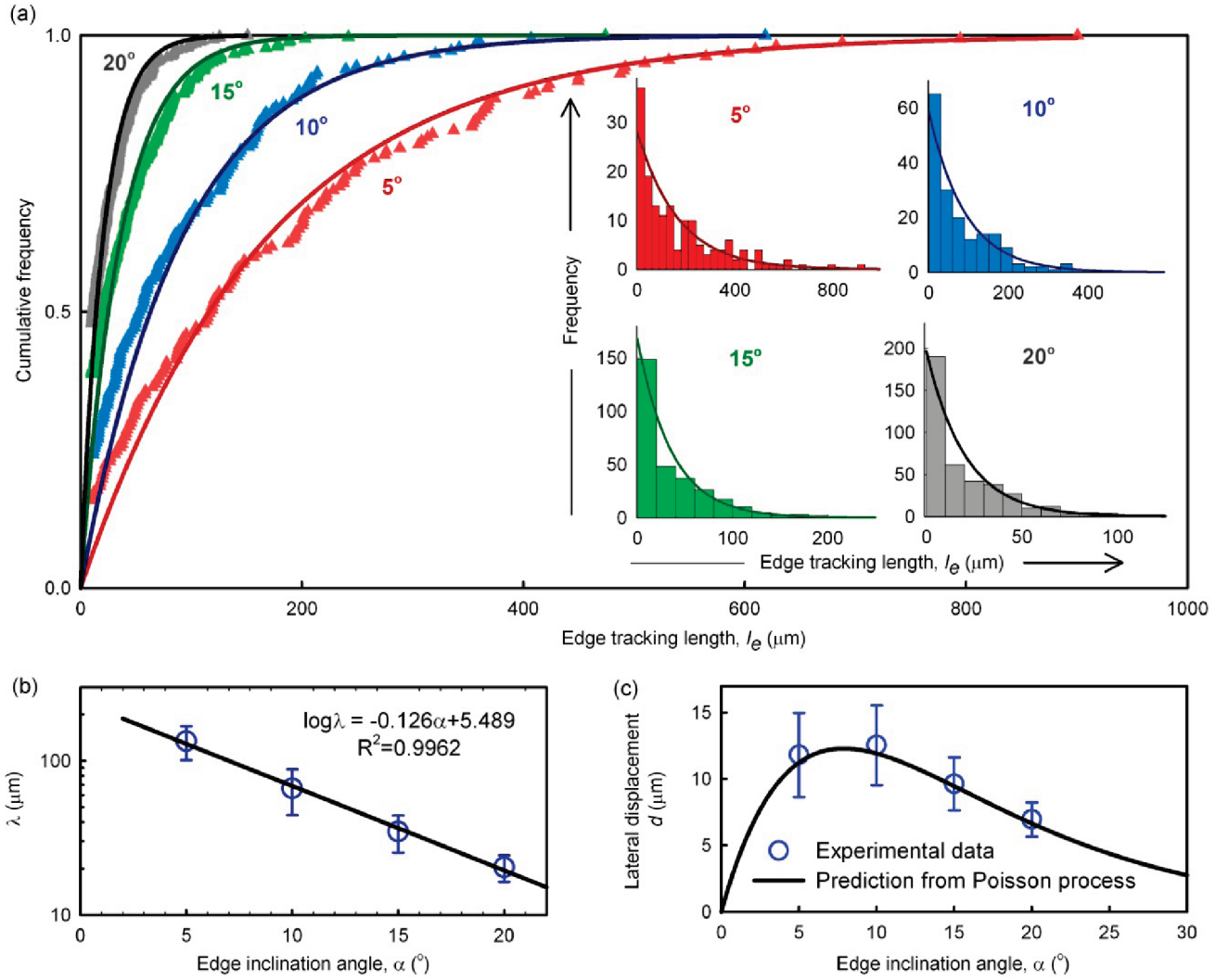

Figure 8. Detachment of cells rolling along an edge can be described by a Poisson distribution. (a) Cumulative distribution function of edge tracking lengths l_e (filled triangles) fitted to a Poisson distribution described by eq 1 (solid lines). Insets show the frequency distribution of the experimentally measured edge tracking lengths, along with that predicted by the Poisson distribution fit to the CDF (solid lines). Colors indicate different inclination angles α of the receptor pattern. Representative results are shown for only one experiment for each α. (b) Variation of the average value of λ with the edge inclination angle can be described by a linear fit to a semilog plot (solid line). (c) Variation with the edge inclination angle of the average value of the lateral displacement (solid line) obtained from the empirical fit shown in plot b along with the experimental results (open circles). Error bars in plots b and c represent one standard deviation. The shear stress is 0.5 dyn/cm^2.

the mean value of the edge tracking length. The CDF does not involve any arbitrary bin widths and therefore allows for an objective comparison of the actual distribution of the edge tracking lengths with that predicted for a Poisson process (eq 1). Note that the CDFs displayed in Figure 7 do not begin at the origin because edge tracking lengths of < 10 μm could not be resolved by the present video frame rate and magnification; these unresolved lengths were used to calculate the CDF itself but were not used to fit the Poisson function. The Poisson distribution described by eq 1 well fit the CDF for all edge inclination angles considered, and the mean value of λ obtained by fitting to the CDF also accurately predicted the observed edge tracking length histograms (Figure 8a, inset) at different edge inclination angles. Additionally, to confirm that the process of cells detachment from the edge was indeed a Poisson process for a given cell, we calculated λ under different experimental conditions and compared it to the measured average edge tracking lengths (Table 1). We found a strong correspondence between λ and the average edge tracking length from the experiments; even at different shear stress magnitudes, we found the maximum difference to be within 7% (data not shown). As an additional confirmation, we also manually compared the edge tracking lengths for several cells that exhibited multiple rolling and rebinding events within a single experiment; we found no correlation between the initial and subsequent l_e for such cells, as would be expected for a history-independent detachment process (data not shown). These data strongly suggest the fact that the detachment of these HL60 cells rolling along an edge is indeed a random process.

Table 1. Comparison of the Experimental and Poisson Average Values of λ[a]

edge angle	Poisson mean, $\lambda \pm$ SD (μm)	experimental average, $l_e \pm$ SD (μm)	% error, $100(\lambda - l_e)l_e$ (μm)
5	134.1 ± 33.2	135.5 ± 36.3	−0.98
10	66.2 ± 21.7	72.2 ± 17.2	−8.35
15	34.7 ± 9.4	37.2 ± 7.6	−6.60
20	20.3 ± 3.9	20.3 ± 3.7	0.11

[a] n = 3 replicate experiments. Data were obtained by fitting to a Poisson distribution with experimentally measured average edge tracking length l_e. The shear stress is 0.5 dyn/cm^2.

Interestingly, we observed that the average value of λ obtained by fitting the CDF to the Poisson distribution showed an exponential decrease with increasing edge inclination angle (Figure 8b). This observation provides an empirical relationship between the edge angle and the average edge tracking length, and the distribution of the lengths can be modeled using a Poisson process. Thus, this exponential dependence combined with modeling cell detachment as a Poisson process can be used to interpolate the average edge tracking length as well as its distribution for any edge angle between 5 and 20°. We also predict the variation of lateral displacement with the edge inclination angle based on this exponential fit, which agreed well with the experimental data (Figure 8c). Interestingly, the curve predicts an optimal edge inclination angle of between 5 and 10° that maximizes the lateral displacement for rolling along a single edge. This prediction explains why a statistically significant difference was not observed between lateral displacements at edge inclination angles of 5 and 10° (Figure 5).

Prediction of Cell Trajectories on a Receptor-Patterned Substrate. The experimental results obtained in this study enable us to develop a simulation tool for predicting the trajectories and distribution of cells rolling across a substrate patterned with asymmetric P-selectin lines. Here, we incorporate the experimental observations and Poisson process of detachment to simulate the lateral displacement of HL60 cells as they encounter multiple edges of P-selectin. We first compare the simulations with experimental results where the cells encountered three consecutive lines and then simulate the distribution of cells introduced at a downstream location for different edge inclination angles.

We performed a Monte Carlo simulation for 10^5 cells and predicted their displacement after they rolled on three consecutive lines on a 20° edge inclination angle (λ = 20.3 μm) and then compared this displacement to that observed in a single experiment as described in the Data Analysis section (Figure 9a). We found that the simulated results agreed well with the experimental distribution despite the small number of experimental data points available. Although a comparison of the distribution over more edges is desirable, we were limited by the field of view of the camera that could accommodate only approximately three edges of the patterned bands.

Next we performed a Monte Carlo simulation to examine the spreading of cells that are injected at a particular location (0, 0) on a patterned surface (similar to Figure 1a). In the simulation study, the device was assumed to be patterned with parallel P-selectin lines having a width of 50 μm and a gap of 70 μm between adjacent lines (similar to the pattern used in experiments). In addition to the rolling behavior of cells on the P-selectin regions, the reattachment of cells that have detached is an important parameter for predicting the trajectories of cells that encounter several parallel edges. From our experiments, we observed that after detachment from the edge >80% of the cells reattached at the next available downstream P-selectin line at a shear stress of 0.5 dyn/cm^2. Hence, in our simulation we assumed that cells rolled on all of the P-selectin lines that they encountered, with the edge tracking lengths described by a Poisson distribution with the mean λ as obtained earlier.

We performed the simulation for 10^5 cells, and predicted their net lateral displacement and resulting distributions at a longitudinal distance of 1 cm downstream from the origin. Figure 9b summarizes the probability density functions of the net lateral displacement, defined here as the sum of all displacements (analogous to the experimental $l_e \sin\alpha$ in Figure 1a) that a given cell acquired over a longitudinal travel distance of 1 cm. The net lateral displacement increased with increasing edge inclination angle α from 5 to 15°, with little change as α increased from 15 to 20°. The net lateral displacement showed a maximum sensitivity to edge inclination angles of 5 to 10°. This α dependence and sensitivity can be understood as follows. The net lateral displacement was the result of displacements on each edge encountered by the cells. Increasing the edge inclination angle α increases the total number of edges encountered by the cells but simultaneously decreases the mean lateral displacement on each edge ($\lambda\sin\alpha$) (Figure 8c). These opposing effects resulted in the net lateral displacement exhibiting an increase until α = 15° but little change between 15 and 20°. Interestingly, if we assume that the logarithmic dependence of the edge tracking length on α (Figure 8b) is valid at α = 25°, then the net lateral displacement decreases to 152 ± 24 μm, indicating that the effect of the decreasing edge tracking length offsets the effect of the increased edge inclination angle. With an increasing number of edges encountered (i.e., at

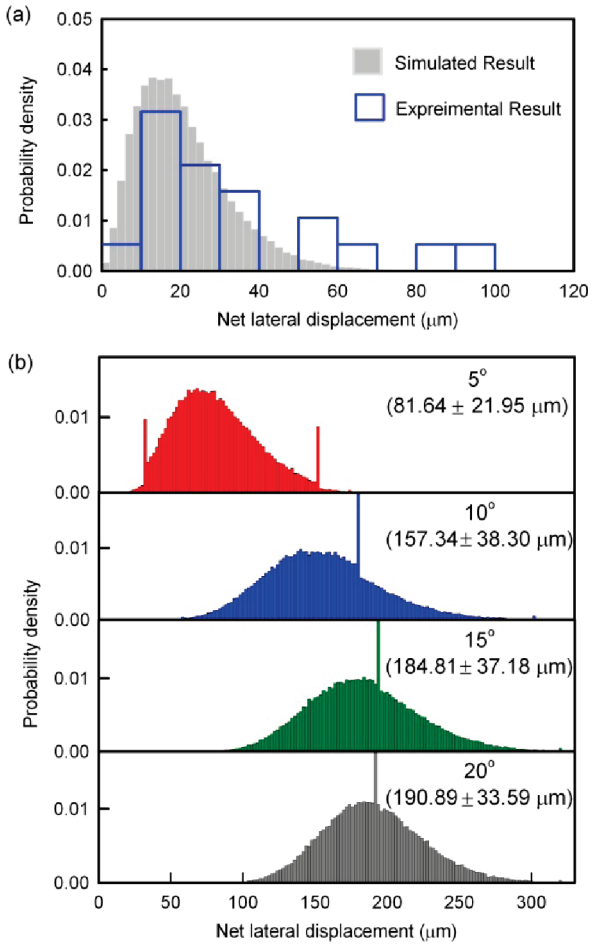

Figure 9. (a) Probability distribution of net lateral displacement of HL-60 cells after rolling on three consecutive lines of P-selectin patterns as obtained from Monte Carlo simulations (shaded area) and experimental observations. α = 20° (shear stress = 0.5 dyn/cm^2). (b) Prediction of the downstream distribution of HL60 cells rolling on patterned P-selectin in a separation device. HL60 cells are introduced at a single location and travel a distance of 1 cm in the downstream direction, interacting with a substrate patterned with P-selectin lines of 50 μm width separated by 70 μm PEG gaps. A net lateral displacement of 10^5 cells was calculated by assuming that detachment on the edge was governed by a Poisson process with parameters as obtained earlier by fitting to experimental data at a shear stress of 0.5 dyn/cm^2. The numbers in parentheses denote the net lateral displacement and standard deviation. The "spikes" appear at the position where the edges intersect the 1 cm downstream position. (The full extent of the spikes is not shown.)

larger α), the distribution of cells is seen to approach a Gaussian distribution, consistent with the central limit theorem. Interestingly, although α = 10 and 20° yield similar net lateral displacements, it is noteworthy that the Gaussian spread is smaller for α = 20°. In fact, the ratio of the mean displacement to the standard deviation increases monotonically from 2.72 to 5.68 as the inclination angle increases from 5 to 20°. This result can again be explained by the fact that the cells undergo more tracking events with increasing α as a result of the greater number of edges per unit length in the direction of flow. It is noteworthy that although the distribution of cells approaches a Gaussian form it is not exactly Gaussian because some of the cells in the distribution are rolling along the edge; these cells create "spikes" in the distribution at specific positions where the edges intersect the axis (at a longitudinal travel distance of 1 cm). Simulations for longitudinal travel lengths of up to 10 cm confirmed that the mean lateral displacement remained proportional to the longitudinal distance traveled by the cells, although the spread in the distribution increased, being approximately proportional to the square root of the downstream distance as is typical of chromatographic separation (data not shown). These results demonstrate that a microfluidic device based on asymmetric receptor patterns can be used for the efficient modulation of cell rolling trajectories, as required for the flow-based separation of cells. From the distributions in Figure 8, it can be predicted that a 100-μm-wide stream of a heterogeneous mixture of receptor-binding and nonbinding cells can be separated for a receptor pattern of α = 20° and device of length 1 cm, provided the solution is dilute enough to minimize dispersion due to cell−cell interactions.

Conclusions

We have designed substrates with multiple P-selectin patterns by a facile, versatile method utilizing microcontact printing. These substrates were incorporated into a flow chamber to study HL60 cell rolling behavior, including the quantification of edge tracking lengths and cell rolling velocities. Among the parameters that we considered, the pattern edge inclination angle modulated the cell rolling trajectory most strongly; in fact, the edge tracking length decreased exponentially with increasing edge inclination angle. In addition, the nature of cell rolling and detachment along the edge was consistent with the Poisson process. This correlation suggests that the detachment of rolling cells from receptor-functionalized edges is a random process that is not disrupted measurably by cell−surface interactions (e.g., pattern biofouling or transmembrane ligand redistributions) over the device timescales considered. An experimental characterization of cell rolling enabled the development of a computational Monte Carlo tool to simulate the trajectories of cells. These simulations indicated that cell separation may be achieved within a short (centimeter-scale) separation channel and also provided a potentially useful approach to optimizing pattern geometry to maximize the cell separation efficiency. The increasing resolution obtained by multiple tracking events on parallel edges indicates that small differences in rolling behavior can be amplified and resolved by increasing the longitudinal traveling distance or the number of edges encountered by the cells, analogously to other analytical processes. Because the cell rolling behavior depends on the ligand density on the cell (among several other parameters), we hypothesize that different cell phenotypes can be separated or identified on the basis of difference in their characteristic lateral displacements. Although the present work does not directly address the feasibility of separating different types of cells that interact with a given selectin receptor, it lays the groundwork for future studies in this direction by elucidating the statistical nature and effect of the edge inclination angle on cell rolling along patterned edges. The ultimate goal is to develop devices that incorporate asymmetric receptor patterns for point-of-care diagnostic and therapeutic applications where rapid cell sorting or analysis with minimal cell processing would be beneficial. Our work indicates the feasibility of realizing such devices and also provides quantitative tools for future device design.

Acknowledgment. This project was supported by the Deshpande Center for Technological Innovation at MIT (R.K. and J.M.K.) and an NSF CAREER award (0952493) to R.K. through the Chemical and Biological Separations program. This work was also partially supported by National Institutes of Health grants DE019191, HL095722, and HL097172, and by American Heart Association grant 0970178N to J.M.K. We thank the Institute for Soldier Nanotechnologies (ISN) and the Microsystems Technology Laboratory (MTL) at MIT for the use of their facilities.

Supporting Information Available: Video of HL60 cells rolling on asymmetric P-selectin patterns. This material is available free of charge via the Internet at http://pubs.acs.org.